

# New Design Criteria for Gusset Plates in Tension

STEVE G. HARDASH and REIDAR BJORHOVDE

Gusset plates are common fastening elements used in fabricated steel structures such as trusses or braced-frame structures. In the latter case, their primary purpose is to transfer either tensile or compressive loads from a bracing member to a beam and column joint.

Current gusset plate design is based primarily on elastic analyses for determining critical sections and stresses. No known failures or adverse behavior have been noted, but substantial differences in the factor of safety against ultimate load exist because of the assumptions involved.<sup>7</sup> Therefore, it is important to develop an improved design method, with the goal of providing economy of design and consistent levels of safety.

The ultimate-strength approach fulfills these requirements. To date, a few experimental studies have been conducted to determine the behavior and ultimate strength of gusset plate connections. However, additional tests have been needed to develop a design method based on ultimate strength behavior. It is the purpose of this paper to describe a number of gusset plate tests that were performed, and to develop rational criteria that incorporate all of the primary strength parameters.

## PREVIOUS WORK

One of the first significant elastic experimental studies of gusset plates was conducted by Whitmore on a Warren truss joint.<sup>19</sup> Analyses showed the maximum tensile and compressive stresses were located in a region of the plate at the ends of the tension and compression diagonals, respectively. It was determined the well-known effective width could be used to define the section subjected to maximum normal stress. Additional elastic

analyses verified the locations of maximum normal stress in the gusset plate are located in a region near the ends of the connected members.<sup>7</sup>

Relatively few ultimate strength tests have been performed of gusset plate connections. The probable reason is that behavior beyond the elastic range could not be determined before the advent of finite element techniques. Chesson and Munse<sup>4</sup> conducted ultimate strength tests of 16 large truss-type connections. Only one of these failed at the gusset, which exhibited tearing across and on the outer lines of bolts. Further work by the same investigators<sup>5</sup> provided ultimate strength data for 30 truss-type tensile connections. In this study, 10 connections failed by tearing in the vicinity of the bolted or riveted connection to the gusset plate.

More recently, tests were conducted at the University of Alberta<sup>3</sup> to determine the ultimate strength of gusset plates used in diagonal bracing connections. The three gusset plates tested to failure were full-sized; tearing was observed across the last row of bolts and also in the boundary connections, along with plate buckling.

Nonlinear finite element analyses of gusset plate behavior have been conducted in recent years.<sup>14,18</sup> The results confirm the maximum normal stresses are located in a region near the end of the gusset plate connection.

## THE BLOCK-SHEAR CONCEPT

In 1976, the Research Council on Riveted and Bolted Structural Joints (now the Research Council on Structural Connections) increased the allowable bearing stress in high-strength bolted joints from  $1.35 F_y$  to  $1.5 F_u$ ,<sup>12</sup> where  $F_y$  and  $F_u$  are the yield and ultimate tensile stresses of the material in the connected parts, respectively. This was a radical alteration that prompted significant changes in the connection design and detailing practices that had been used previously. For example, for ASTM A36, the most commonly used grade of steel for construction purposes, the increase in the bearing stress amounted to approximately 80%, from 48.6 ksi to 87.0 ksi (335 MPa to 600 MPa).

---

Steve G. Hardash is a Structural Engineer, Robin E. Parke & Associates, Phoenix, Arizona; and formerly graduate student, University of Arizona, Tucson, Arizona.

Reidar BJORHOVDE is Professor of Civil Engineering and Engineering Mechanics, University of Arizona, Tucson, Arizona.

---

Around the time when the changes in the bearing stress criteria were implemented, research was conducted at the University of Toronto on the shear force capacity of coped beam webs. This work had been undertaken to verify the shear design criteria of the new Canadian limit states design standard.<sup>17</sup> The research involved a series of full-scale tests on uncoped and coped double-angle beam-to-column connections, loaded in as close to pure shear conditions as possible.<sup>2</sup> Beam action therefore did not enter into the overall behavior of the connection.

It was found the coped web failed in a mode that involved a combination of a horizontal splitting of the beam web at the lower bolt hole, along with an elongation of all bolt holes in the direction parallel to the applied force. This produced a shearing out of a block of the web, as in Fig. 1, leading to the development of the concept of a block-shear ultimate strength model. In the block-shear model, the strength is developed by the shear resistance of the web along line 1-1 (see Fig. 1), in addition to the tensile resistance of the web along line 2-2.

As a result of the above studies, the AISC Specification<sup>12</sup> incorporated design criteria for connections aimed at covering the block-shear problem. The allowable strength is thus given by Eq. 1 as:

$$R_a \leq 0.30 A_v F_u + 0.50 A_t F_u \quad (1)$$

where:

$R_a$  = allowable resistance to block-shear, kips

$A_v$  = net shear area along line 1-1, in.<sup>2</sup>

$A_t$  = net tension area along line 2-2, in.<sup>2</sup>

$F_u$  = specified minimum tensile strength, ksi.

This equation is based on a factor of safety against tension failure of 2.0 (hence,  $0.5 F_u$ ), and against shear failure of approximately 2.0. It is implied that the ultimate shear stress is related to the ultimate tensile stress as  $0.6 F_u$ .

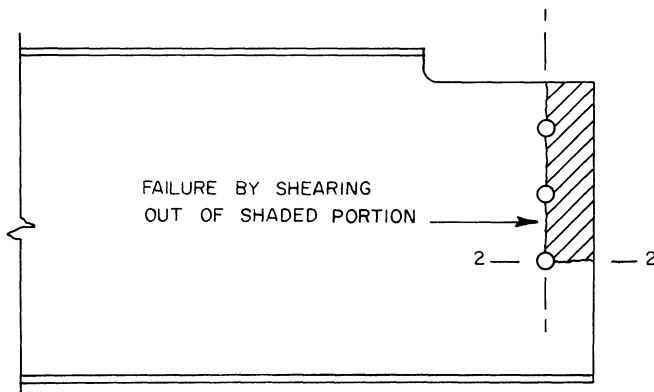


Fig. 1. Block-shear model of failure for coped-beam web

Further testing of coped beam connections was conducted at the University of Texas at Austin. The findings were used to develop modifications to the original block-shear model.<sup>16,20</sup>

Based on the work with coped beam-to-column connections, the block-shear failure mode has been considered for application to gusset plates loaded in tension. One such suggestion was advanced by the AISC Commentary;<sup>12</sup> subsequent evaluations of full-size gusset plate tests<sup>3,15</sup> suggested a model in which the ultimate shear resistance was developed along the last row of bolts, as shown in Fig. 2. The agreement between tests and theory was good; a maximum error of 7% was recorded.

Since this initial application of the block-shear concept to gusset plates only involved diagonal bracing gusset plates whose block-shear strength parameters were limited, it would appear to be necessary to further modify the model to take into account all of them. Thus, factors such as connection length, distance between outside bolt lines, plate thickness, bolt diameter, material yield and ultimate strengths and the plate geometry should be considered. This has been accomplished in the investigation presented in this paper.

#### EXPERIMENTAL STUDIES OF GUSSET PLATES

To develop an ultimate strength approach to the design of gusset plates, a series of gusset plate tests was conducted at the University of Arizona.<sup>11</sup> In addition, the

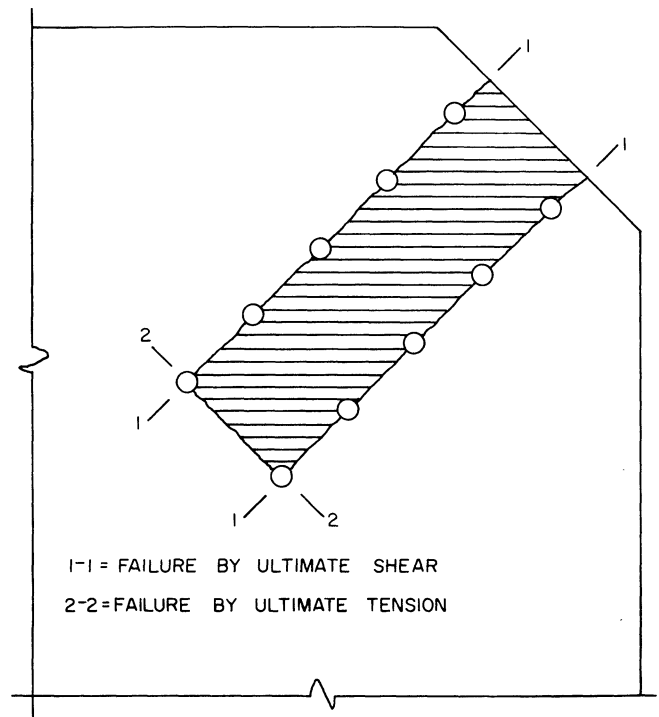


Fig. 2. Suggested block-shear model for gusset plates

results of the work conducted at the University of Illinois<sup>4,5</sup> and the University of Alberta<sup>3</sup> have been incorporated into the strength evaluations. Details of each of the testing programs are given in the following.

### University of Arizona

To evaluate the application of the block-shear concept to gusset plate behavior and design, it was decided to test plates loaded in tension through two lines of bolts.<sup>11</sup> The intent was to isolate the tested joint so as to observe its behavior. Figure 3 shows the general configuration of the gusset plate. The region of interest is delineated by the measurements  $l$  and  $S$ .

As indicated in the figure, the following were considered as the strength parameters for the plates: (1) gage between lines of bolts,  $S$ ; (2) edge distance,  $e$ ; (3) bolt pitch,  $s$ ; and (4) number of bolts. The total connection length  $l$  depends on the edge distance and the total number of bolts in a line.

A total of 28 gusset plates were tested, using  $S$ -values of 2, 3 and 4 in. (51, 76 and 101 mm), 1 and 1½ in. (25 and 38 mm) for  $e$ , and 1½ and 2 in. (38 and 51 mm) for  $s$ . The bolts used for all the tests were ½ in. (13 mm) diameter ASTM A325, and the number of bolts in a line ranged from 2 to 5.

Material properties of the plate steel were determined by tension coupon tests, performed in accordance with the procedures of ASTM 370.<sup>1</sup> Due to a fabrication mix-

up, one plate was fabricated from a different steel grade. The average material properties were as follows: For tests plates Nos. 1 to 17 and 19 to 28,  $F_y = 33.2$  ksi (229 MPa) and  $F_u = 46.9$  ksi (323 MPa);

For test plate No. 18,  $F_y = 49.5$  ksi (341 MPa) (0.2% offset) and  $F_u = 64.5$  ksi (444 MPa).

Slight fabrication errors required that test connection holes be redrilled to a diameter of 11/16 in. (17.5 mm) [3/16 in. (5 mm) oversize] for three of the test specimens (Nos. 16, 20 and 26). However, neither of these changes had any effect on the strength model that was developed.

The gusset plate tests were performed using a 200-kip capacity Tinius-Olsen universal testing machine. Load-deformation data were obtained by positioning a dial gage between the testing machine crossheads, with deformation readings recorded at convenient load increments. The final test set-up is shown schematically in Fig. 4, and a photograph of an installed and instrumented plate in Fig. 5. Details of the failure loads, connection geometries and material properties for the tested gusset plates are given in Table 1.

All of the gusset plates behaved similarly, reflecting the following characteristics: (1) slip took place during

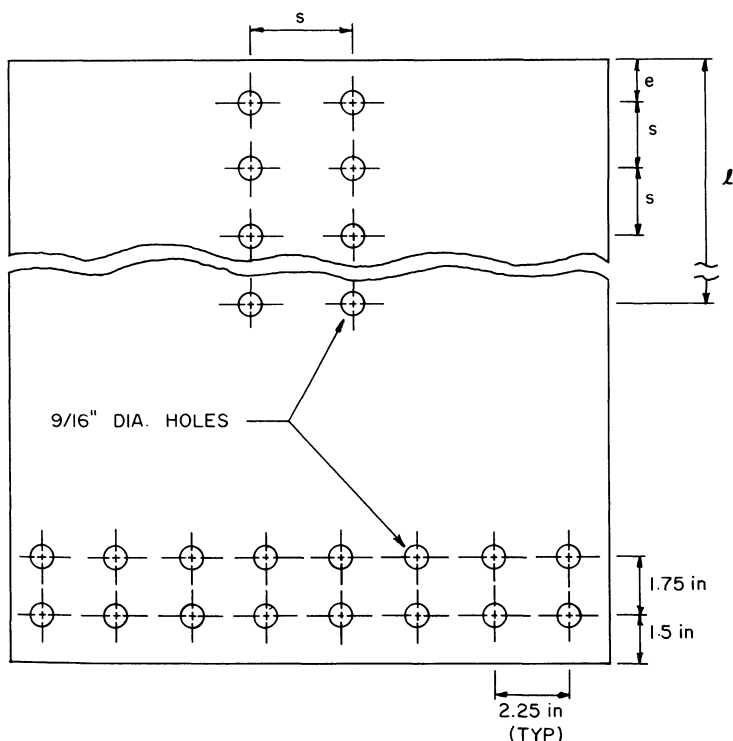


Fig. 3. General gusset test plate configuration

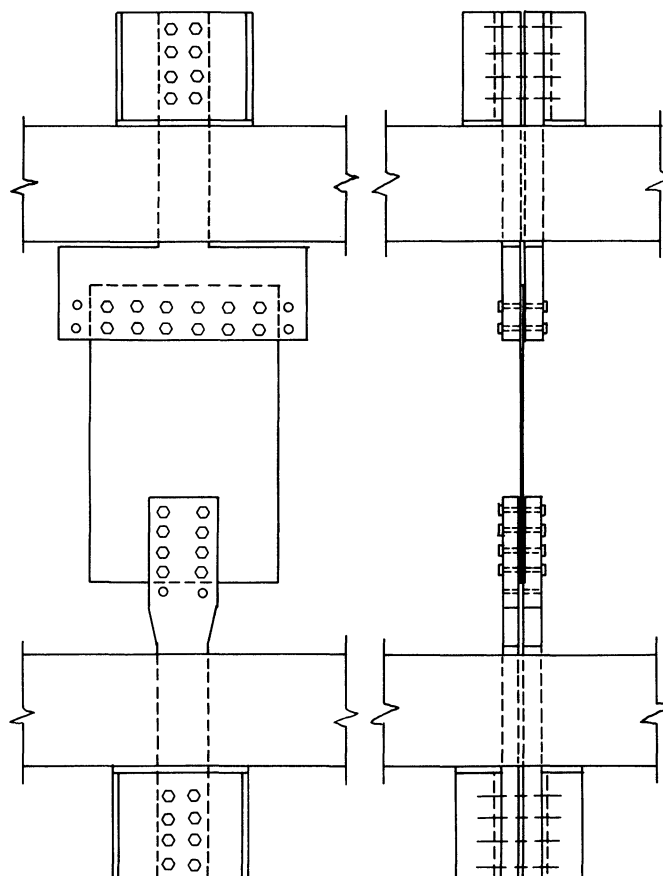


Fig. 4. Front and side view of typical test setup

Table 1. Gusset Plate Test Data (University of Arizona Study<sup>11</sup>)

| Test No. | $P_{ult}$ (kips) | Hole Dia. (in.) | $S$ (in.) | $e$ (in.) | $s$ (in.) | $l$ (in.) | $t$ (in.) | $F_y$ (ksi) | $F_u$ (ksi) |
|----------|------------------|-----------------|-----------|-----------|-----------|-----------|-----------|-------------|-------------|
| 1        | 54.6             | 9/16            | 2.00      | 1.10      | 1.50      | 2.60      | 0.237     | 33.2        | 46.9        |
| 2        | 55.2             | 9/16            | 2.00      | 1.50      | 1.50      | 3.00      | 0.237     | 33.2        | 46.9        |
| 3        | 67.6             | 9/16            | 2.00      | 1.00      | 2.00      | 4.00      | 0.237     | 33.2        | 46.9        |
| 4        | 73.6             | 9/16            | 2.00      | 1.00      | 2.00      | 5.00      | 0.237     | 33.2        | 46.9        |
| 5        | 71.5             | 9/16            | 2.00      | 1.50      | 1.50      | 4.50      | 0.237     | 33.2        | 46.9        |
| 6        | 81.1             | 9/16            | 2.00      | 1.50      | 2.00      | 5.50      | 0.237     | 33.2        | 46.9        |
| 7        | 76.2             | 9/16            | 3.00      | 1.00      | 1.50      | 4.00      | 0.237     | 33.2        | 46.9        |
| 8        | 83.4             | 9/16            | 3.00      | 1.00      | 2.00      | 5.00      | 0.237     | 33.2        | 46.9        |
| 9        | 80.6             | 9/16            | 3.00      | 1.50      | 1.50      | 4.50      | 0.237     | 33.2        | 46.9        |
| 10       | 89.9             | 9/16            | 3.00      | 1.50      | 2.00      | 5.50      | 0.237     | 33.2        | 46.9        |
| 11       | 84.2             | 9/16            | 4.00      | 1.00      | 1.50      | 4.00      | 0.237     | 33.2        | 46.9        |
| 12       | 91.6             | 9/16            | 4.00      | 1.60      | 1.50      | 4.60      | 0.237     | 33.2        | 46.9        |
| 13       | 79.5             | 9/16            | 2.00      | 1.00      | 2.00      | 5.50      | 0.237     | 33.2        | 46.9        |
| 14       | 95.0             | 9/16            | 2.00      | 1.00      | 2.00      | 7.00      | 0.237     | 33.2        | 46.9        |
| 15       | 85.2             | 9/16            | 2.00      | 1.50      | 1.50      | 6.00      | 0.237     | 33.2        | 46.9        |
| 16       | 99.8             | 11/16           | 2.00      | 1.50      | 2.00      | 7.50      | 0.237     | 33.2        | 46.9        |
| 17       | 88.1             | 9/16            | 3.00      | 1.00      | 1.50      | 5.50      | 0.237     | 33.2        | 46.9        |
| 18       | 154.5            | 9/16            | 3.00      | 1.00      | 2.00      | 7.00      | 0.253     | 49.5        | 64.5        |
| 19       | 92.9             | 9/16            | 3.00      | 1.50      | 1.50      | 6.00      | 0.237     | 33.2        | 46.9        |
| 20       | 119.7            | 11/16           | 3.00      | 1.50      | 2.00      | 7.50      | 0.237     | 33.2        | 46.9        |
| 21       | 105.0            | 9/16            | 4.00      | 1.00      | 1.50      | 5.50      | 0.237     | 33.2        | 46.9        |
| 22       | 114.9            | 9/16            | 4.00      | 1.00      | 2.00      | 7.00      | 0.237     | 33.2        | 46.9        |
| 23       | 109.6            | 9/16            | 4.00      | 1.50      | 1.50      | 6.00      | 0.237     | 33.2        | 46.9        |
| 24       | 118.0            | 9/16            | 3.00      | 1.65      | 2.00      | 7.65      | 0.237     | 33.2        | 46.9        |
| 25       | 105.1            | 9/16            | 3.00      | 1.00      | 1.50      | 7.00      | 0.237     | 33.2        | 46.9        |
| 26       | 131.2            | 11/16           | 3.00      | 1.00      | 2.00      | 9.00      | 0.237     | 33.2        | 46.9        |
| 27       | 112.0            | 9/16            | 3.00      | 1.50      | 1.50      | 7.50      | 0.237     | 33.2        | 46.9        |
| 28       | 125.7            | 9/16            | 3.00      | 1.50      | 2.00      | 9.50      | 0.237     | 33.2        | 46.9        |

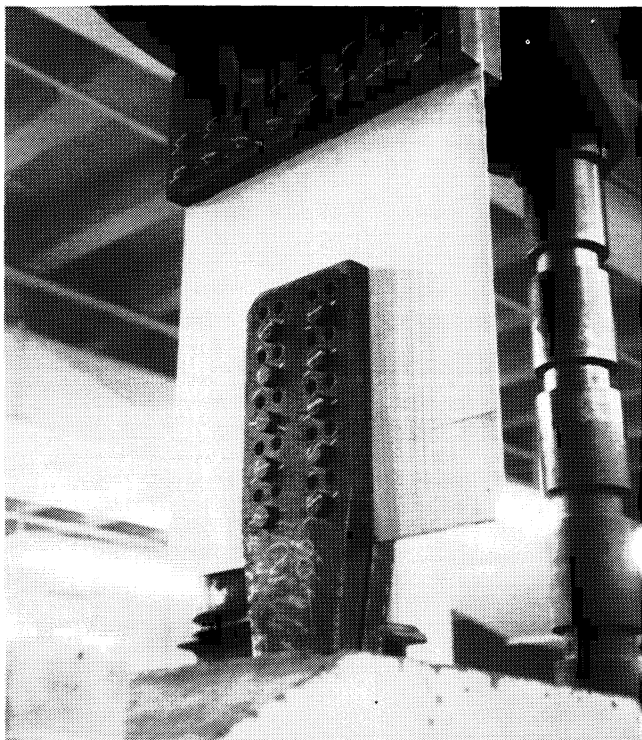


Fig. 5. Test setup with plate No. 28 installed

the elastic loading phase; (2) the plates exhibited a long yield plateau to ultimate load; and (3) the load subsequently dropped to a second strength plateau. As an example, a typical load-deformation curve is that for test plate No. 28, shown in Fig. 6.

Out of the 28 gusset plates tested, 12 exhibited some slipping during the elastic loading portion of the load-deformation curve. As the loading progressed, it was found the occurrence of the first yield lines accurately signaled the beginning of the yield plateau on the load-deformation curve. After reaching the ultimate strength, recording of the load-deformation data was continued until the load was stabilized at a second (lower) strength plateau. This plateau would be reached when the tensile failure across the last row of bolts was complete.

The plate failure modes only depended on the types of steel in the plate, as shown in Fig. 7. For the test plates fabricated of mild structural steel (test specimen Nos. 1 to 17 and 19 to 28), the basic failure mode consisted of a tensile failure across the last row of bolts, along with an elongation of the bolt holes, as shown in Figs. 7a and 8b. None of the test specimens showed significant tearing across the lines of bolts in the direction of the applied load. Oversizing the connection holes (test plate Nos. 16, 20 and 26) did not influence the failure mode for this type of steel. For test specimen No. 18,

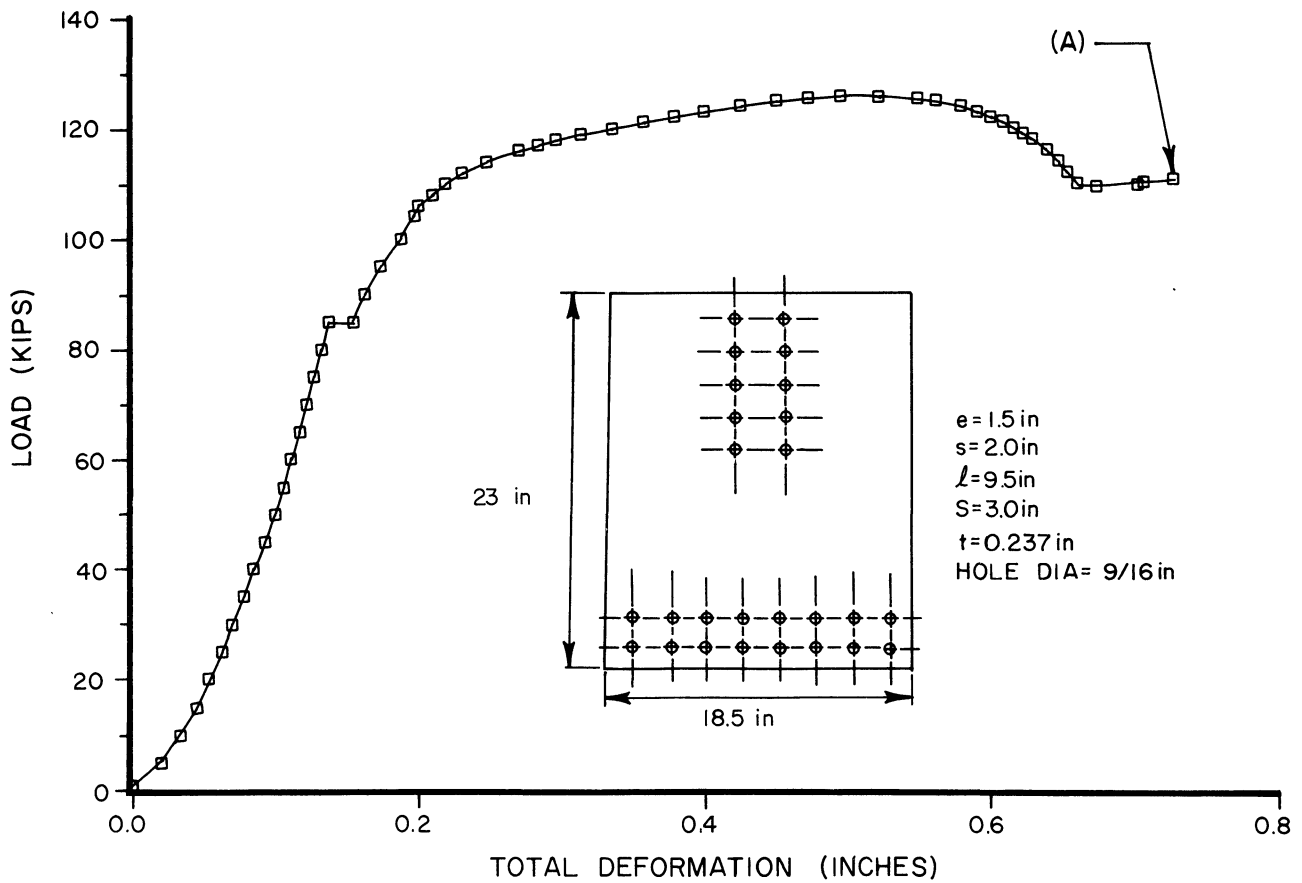
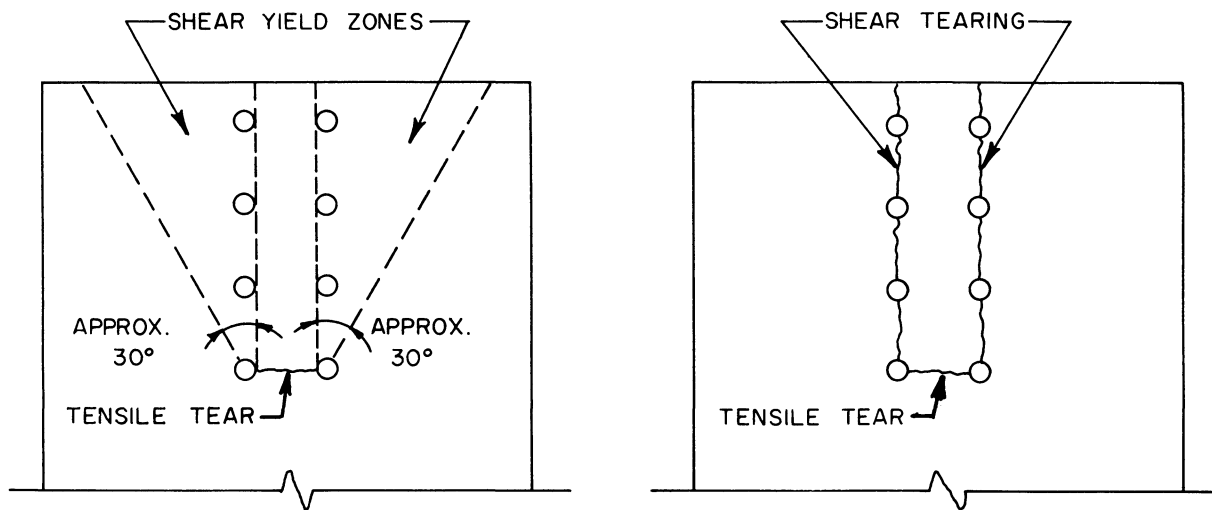


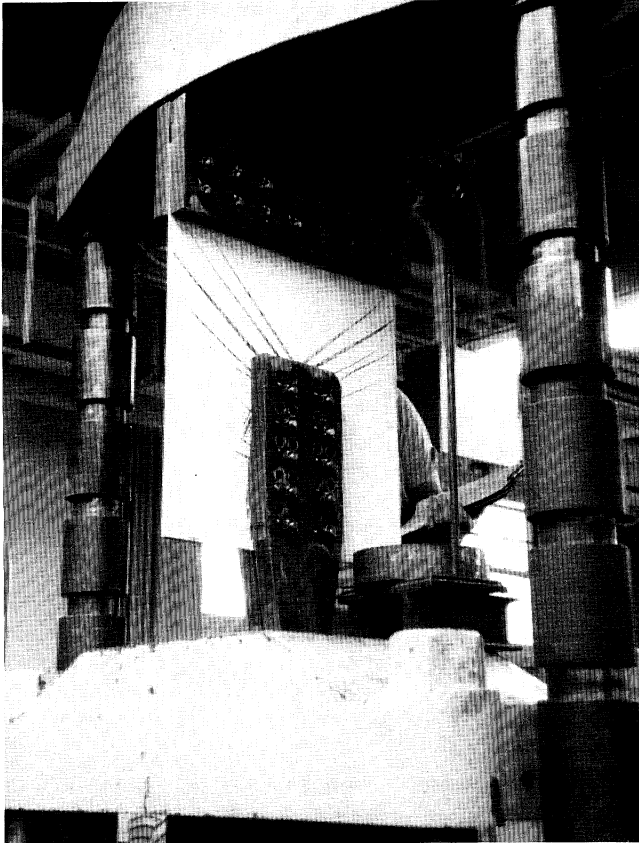
Fig. 6. Load-deformation curve for test plate No. 28



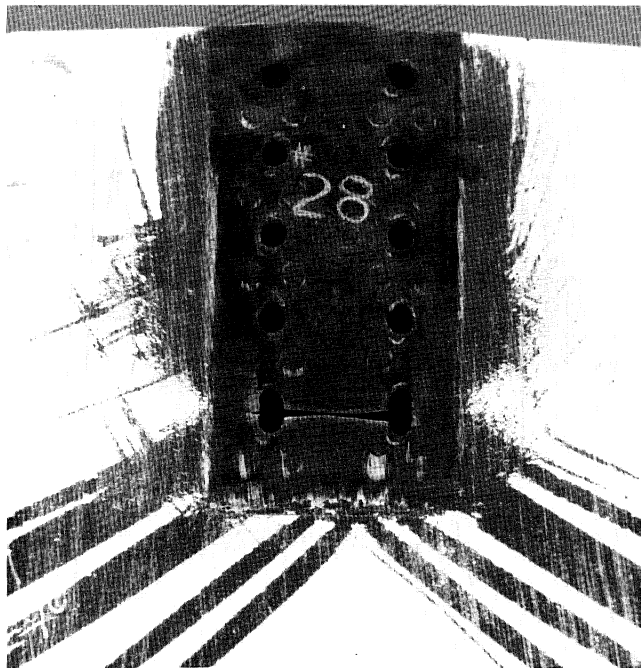
(a) Tensile failure with shear yielding (mild, hot-rolled structural steel)

(b) Tensile failure with shear tearing (cold-rolled structural steel)

Fig. 7. Two basic failure modes for gusset test plates



(a)



(b)

Fig. 8. Test plate No. 28 at end of loading cycle  
 (a) Load = 110 kips (point A on curve of Fig. 6)  
 (b) Specimen removed from the testing machine

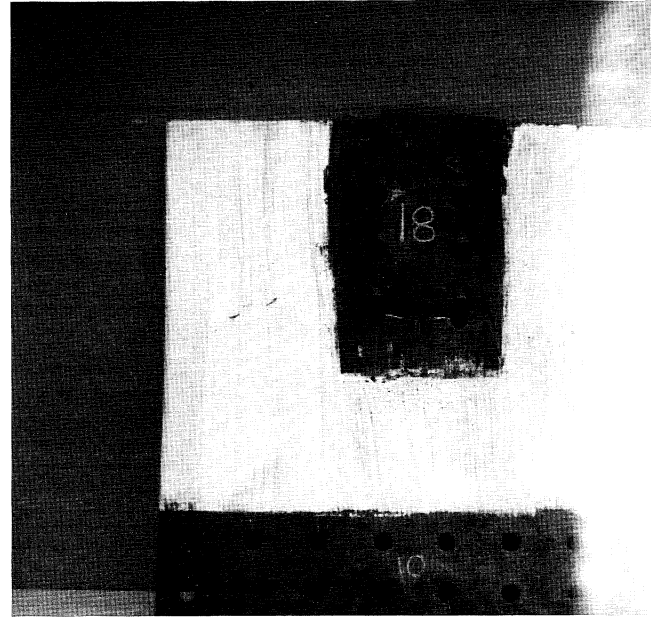


Fig. 9. Test plate No. 18 at end of loading cycle

fabricated from cold-rolled structural steel, the failure mode also included the tearing across the last row of bolts. However, along with the elongation of the bolt holes, the specimen also exhibited some tearing along the bolt lines as indicated by Figs. 7b and 9. It was observed during the testing that the shear failure along the bolt lines occurred after the ultimate load was reached.

#### University of Illinois

The 1958 study<sup>4</sup> resulted in only one connection failure at the gusset plates, and the 1963 study<sup>5</sup> gave 10 additional sets of data. These tests incorporated riveted and bolted joints in either single- or double-plane connection configurations. Two gusset plate connections consisted of 5 lines of bolts with 7 bolts per line; this gave a total distance between outside bolt lines of 12 in. (305 mm) and a total connection length of 17 in. (432 mm). The remaining test connections had 2 lines of bolts, with either 7 or 10 bolts per line; the overall connection length was either 19<sup>1</sup>/<sub>4</sub> (489 mm) or 24<sup>1</sup>/<sub>2</sub> in. (622 mm), with the shorter connections having a gage between bolt lines of 4 in. (101 mm). The holes were either punched or drilled, and the influence of these parameters will be examined in the following. Failure modes consisted of tearing across the last row of bolts with some tearing along the bolt lines.

#### University of Alberta

The University of Alberta study<sup>3</sup> yielded three failures of diagonal bracing connection gusset plates. All three

**Table 2. Gusset Plate Test Data for University of Illinois<sup>4,5</sup> and University of Alberta<sup>3</sup> Studies**

| New Test No. | Previous Test No.       | $P_{ult}$ (kips) | Hole Dia. (in.) | $S$ (in.) | $l$ (in.) | $t$ (in.) | $F_y$ (kips) | $F_u$ (kips) |      |
|--------------|-------------------------|------------------|-----------------|-----------|-----------|-----------|--------------|--------------|------|
| 29           | AD1                     | 617.5            | 13/16           | 12.0      | 17.0      | 0.50      | 34.2         | 60.0         |      |
| 30           | A-1-DB <sup>a</sup>     | 640.0            | ↓               | 12.0      | ↓         | ↓         | 36.2         | 59.0         |      |
| 31           | SA-1-PR <sup>a</sup>    | 483.8            |                 | 4.0       |           |           | 34.9         | 61.1         |      |
| 32           | SA-2-PR <sup>a</sup>    | 476.5            |                 | 5.0       |           |           | 42.4         | 55.7         |      |
| 33           | SA-1-PB <sup>a</sup>    | 481.4            |                 | 19.25     |           |           | 0.125        | 42.4         | 55.7 |
| 34           | SA-2-PB <sup>a</sup>    | 482.0            |                 | 24.5      |           |           | 0.50         | 35.9         | 61.8 |
| 35           | SA-2-DB <sup>a</sup>    | 504.1            |                 | 5.25      |           |           | 35.9         | 61.8         |      |
| 36           | 30° Gusset <sup>b</sup> | 142.7            |                 | 5.25      |           |           | 35.9         | 61.8         |      |
| 37           | 45° Gusset <sup>b</sup> | 148.1            |                 | 5.25      |           |           | 35.9         | 61.8         |      |
| 38           | 60° Gusset <sup>b</sup> | 158.4            |                 | 5.25      |           |           | 35.9         | 61.8         |      |
| 39           | SE-1-DR <sup>a</sup>    | 772.0            |                 | 5.25      |           |           | 35.9         | 61.8         |      |
| 40           | SE-2-DB <sup>a</sup>    | 778.0            |                 | 5.25      |           |           | 35.9         | 61.8         |      |
| 41           | SE-1-PR <sup>a</sup>    | 576.0            |                 | 5.25      |           |           | 35.9         | 61.8         |      |
| 42           | SE-2-PR <sup>a</sup>    | 582.0            | 5.25            | 35.9      | 61.8      |           |              |              |      |

<sup>a</sup>For last two letters: D = drilled holes, P = punched holes, R = rivets used in the connection, and B = bolts used in the connection.

<sup>b</sup>Angle measured from the beam axis.

plates had the same geometry for the connection region, which consisted of 2 lines of bolts with 9 bolts per line; the gage between bolt lines was 5 in. (127 mm), with a total connection length of 19<sup>1</sup>/<sub>4</sub> in. (489 mm). However, each plate reflected a different bracing member angle, using inclinations of 30°, 45° and 60° with respect to the beam axis. All three gusset plates failed by tearing of the plate at the last row of bolts in the tension connection, in a direction perpendicular to the applied tensile loads.

Details of the failure loads, connection geometries and material properties for the University of Illinois and the University of Alberta studies are presented in Table 2. It should be noted the test specimens have been re-numbered here, in order of increasing connection length.

### DEVELOPMENT OF ULTIMATE STRENGTH CRITERIA

#### Block-Shear Modeling

The relationship between the ultimate load and the observed failure mode must be considered to develop a strength model that accurately reflects the true behavior at ultimate strength. For a tensile gusset plate connection, it appears the strength model must incorporate two terms: one reflecting the tensile resistance developed at the last row of bolts, and one reflecting the shear resistance developed along the outside bolt lines.

For all 42 gusset plate test specimens, a tensile tear across the last row of bolts was observed, regardless of the strength parameters, hole size or plate material. This suggests that to model the connection behavior accurately, the ultimate strength model must incorporate the ultimate tensile stress of the plate material  $F_u$  over the

area between the two outside bolts in the last row. From the test results for the 28 plates in the present study, it was found the drop in strength from the ultimate load to the second strength plateau corresponded approximately to the ultimate tensile strength of the net area at the last row of bolts. That is, as the plate tore, the load was reduced by the magnitude  $F_u[t(S - d)]$ . This is shown by the schematic load-deformation curve in Fig. 10.

Ultimate shear resistance is more difficult to define, since the shear behavior varied among the 42 test specimens. For instance, the 28 plates of the present study did not display significant tearing along the bolt lines. Only the test plate made from the cold-rolled steel (No. 18) was observed to tear along the bolt lines, but this occurred after the ultimate strength was reached. This suggests the shear stress distribution is not uniform, as

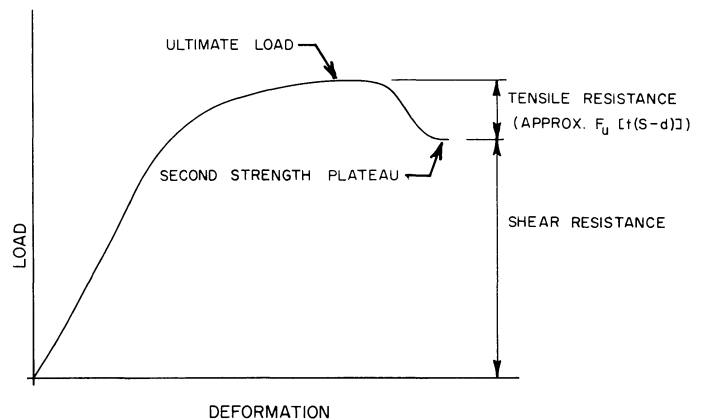


Fig. 10. General load-deformation diagram for gusset plates

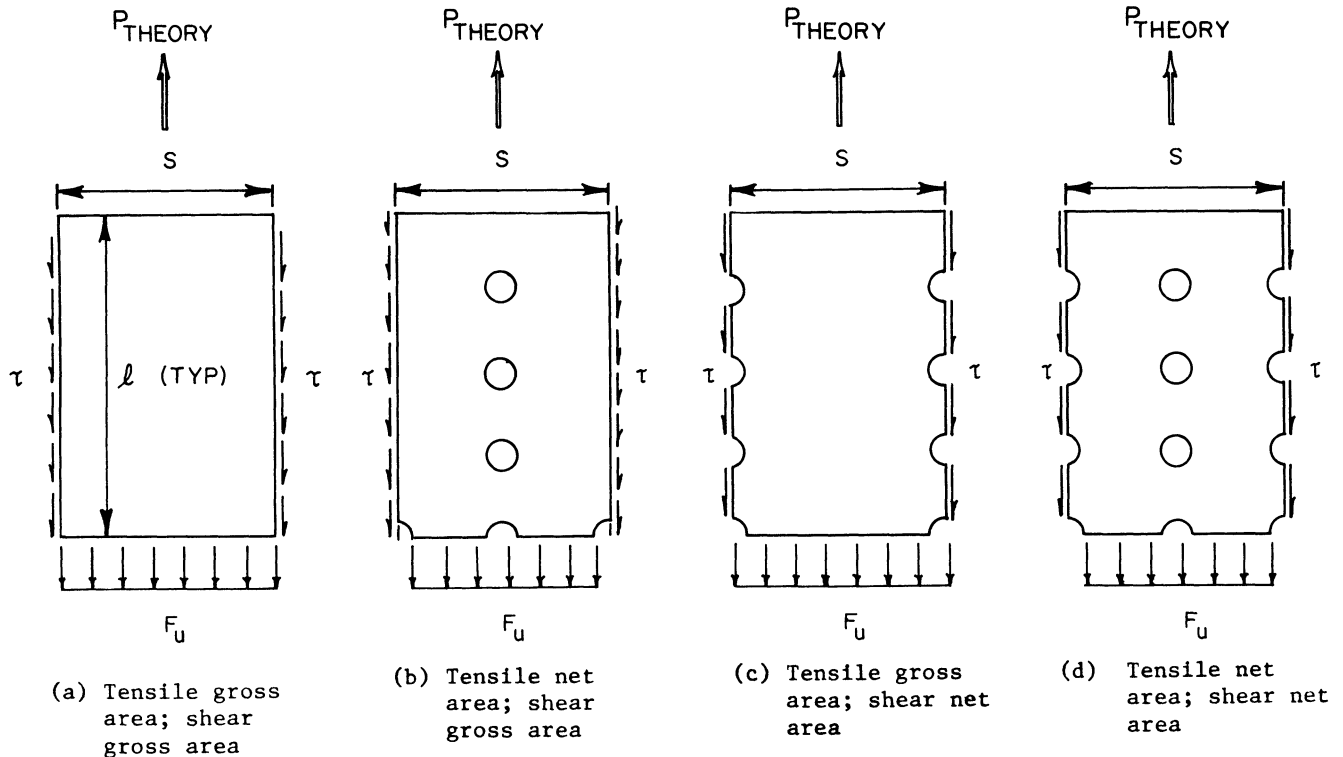


Fig. 11. The four basic free-body sections of gusset plate

has been indicated in early examinations, but rather depends on the particular connection geometry and material.

The contribution of each of these terms (tensile resistance and shear resistance) in the ultimate strength model is shown in Fig. 10.

#### Detailed Block-Shear Model Development

Based on the discussion of the previous section, four basic free body diagrams can be constructed for the connection region; these diagrams are shown in Fig. 11. The basic differences between the four is the method of considering the areas (either gross or net) over which the tensile stress and the shear stress act. The ultimate tensile strength  $F_u$  is the assumed level of stress on the tensile area at ultimate strength. The shear stress  $\tau$  is of unknown magnitude, but is assumed to be distributed uniformly along the shear area.

The shear-yield stress of steel has been determined to lie within the range of one-half to five-eighths of the tensile-yield stress. Using the von Mises yield criterion for plane stress gives the shear-yield stress as  $\tau_y = F_y / \sqrt{3}$ . This relationship is based on a mechanistic failure model for a ductile material such as steel, and will be used in this study. Therefore, the shear stress magnitude used here is  $\tau = F / \sqrt{3}$ , where  $F$  represents an unknown tensile stress.

From the diagrams in Fig. 11, the following equations

describe the ultimate capacity  $P_{theory}$  of the four connection models:

$$1. \text{ Gross-gross: } P_{theory} = F_u S t + 2(F/\sqrt{3})l t \quad (2a)$$

$$2. \text{ Net-gross: } P_{theory} = F_u S_{net} t + 2(F/\sqrt{3})l t \quad (2b)$$

$$3. \text{ Gross-net: } P_{theory} = F_u S t + 2(F/\sqrt{3})l_{net} t \quad (2c)$$

$$4. \text{ Net-net: } P_{theory} = F_u S_{net} t + 2(F/\sqrt{3})l_{net} t \quad (2d)$$

The value for the shear stress  $F/\sqrt{3}$  has purposely been left in general terms to allow for variations of this undefined stress term.

To compare the actual failure loads to those obtained by the models of Fig. 11 and Eq. 2, it is convenient to use the non-dimensional term  $P$ , which is known as the professional factor in Load and Resistance Factor Design (LRFD) terminology.<sup>8,10</sup> The professional factor is an indication of the accuracy of the model and is given by the expression:

$$P = \frac{\text{Test ultimate strength}}{\text{Theoretical ultimate strength}}$$

A value of  $P = 1.0$  would indicate perfect agreement between the strength model and the observed strength.

The results of the test versus theory comparisons for the different connection models are shown in Figs. 12a through d, corresponding to the results using Eqs. 2a through d. In each figure, two extremes of shear stress are used:  $\tau = \tau_y$  and  $\tau = \tau_u$ .

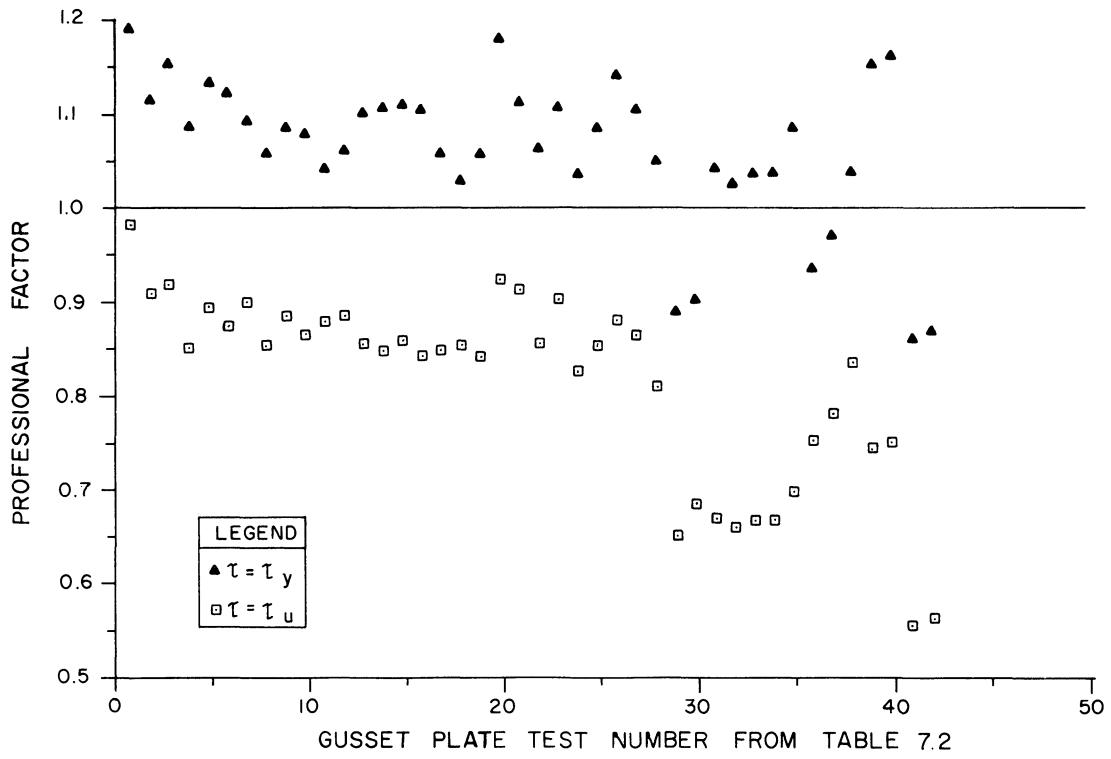


Fig. 12a. Professional factor values, based on tensile gross and shear gross areas

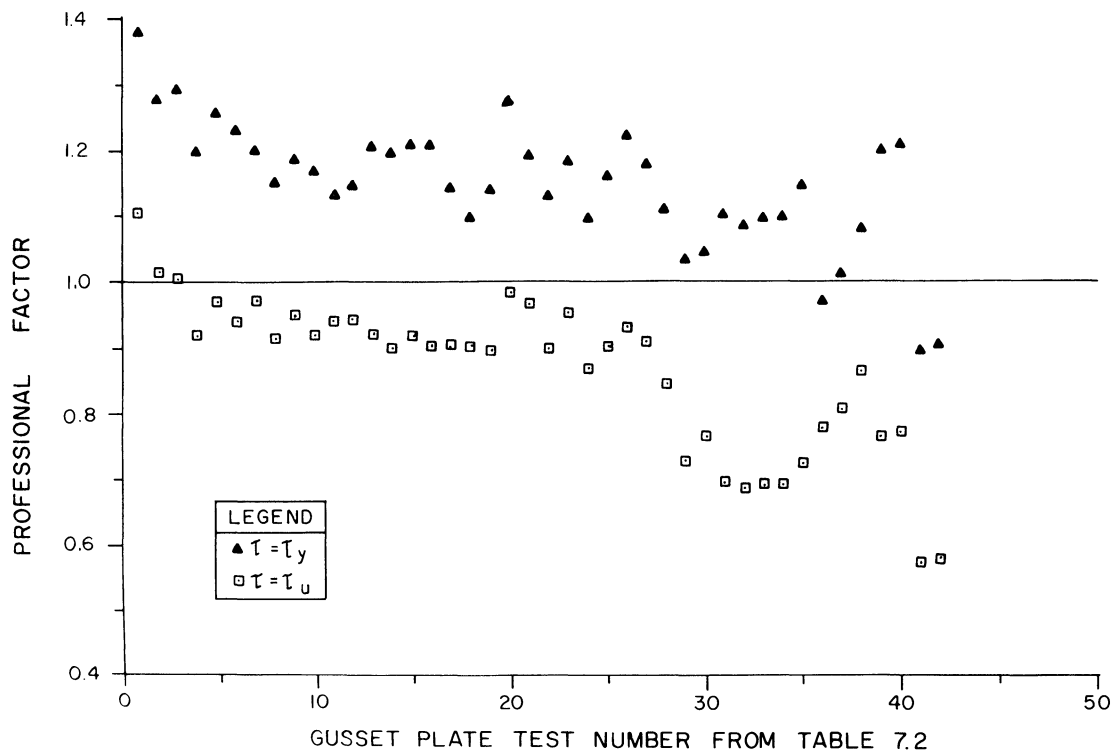


Fig. 12b. Professional factor values, based on tensile net and shear gross areas

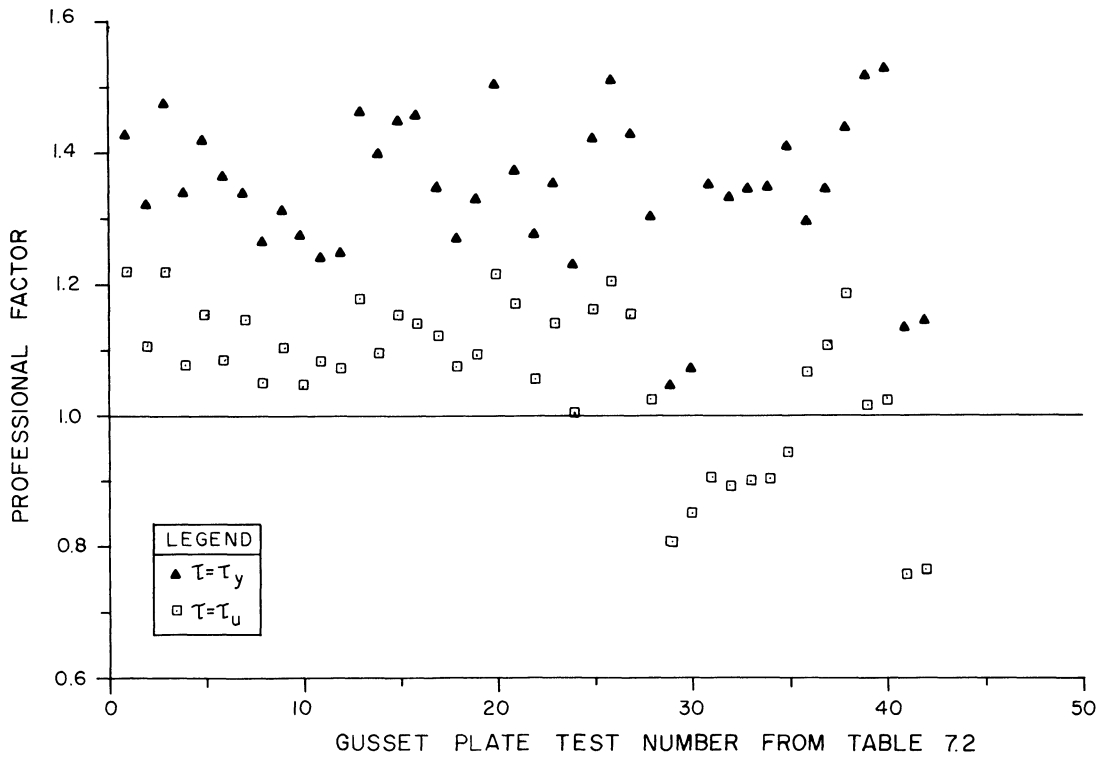


Fig. 12c. Professional factor values, based on tensile gross and shear net areas

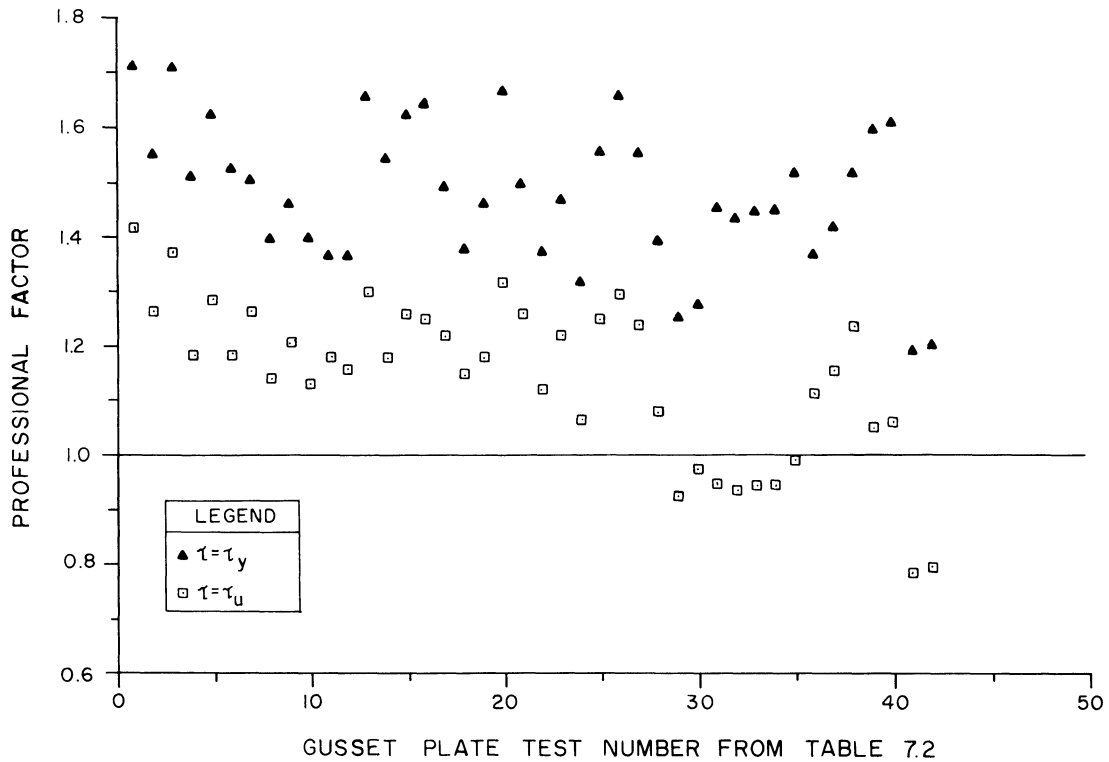


Fig. 12d. Professional factor values, based on tensile net and shear net areas

Figure 12a shows that using the ultimate shear stress value along the bolt lines gives a much larger theoretical failure load (small professional factor), while using the shear yield stress gives a smaller theoretical failure load for the majority of the tests. In Fig. 12b, using the ultimate shear stress appears to work well for the shorter connections (smaller gusset plate test number), while the shear yield stress gives good results for the longer connections. Both Figs. 12c and 12d show that using the net area for the shear effect underestimates the failure load by a large margin for a majority of the test specimens.

The conclusion is that the block-shear model using the net tensile area and the gross shear area, as in Fig. 11b, is the most acceptable. It can also be concluded that, as the gusset plate connection length increases (corresponding to an increasing test specimen number, as they have been arranged), the professional factor decreases. This indicates the effect of varying the connection length is important, and it must be incorporated in a rational and complete gusset plate model.

Figure 12b shows that for short connections, the ultimate shear stress acting on the gross connection length

area would be appropriate, while for longer connections, the tendency is to approach the shear yield stress. This shows the assumed uniformly distributed shear stress must be expressed as a function of the connection length. This can be accomplished by considering an interpolation between the yield and ultimate shear stress, expressed in terms of the tensile stress ( $\tau_{eff} = F_{eff}/\sqrt{3}$ ), as the following:

$$F_{eff} = (1 - C_l)F_y + C_lF_u \quad (3)$$

where:

$F_{eff}$  = Effective tensile stress

$C_l$  = Connection length factor

The variable  $C_l$  is the linear interpolation factor; if  $C_l$  equals zero, then  $F_{eff}$  equals the tensile yield stress, and if  $C_l$  equals one, then  $F_{eff}$  equals the tensile ultimate stress.

Using the net tensile area-gross shear area block-shear model, it is possible to determine the required value for  $C_l$  to give exact agreement with the observed ultimate strength for each test. Figure 13 illustrates this result as a function of the connection length  $l$ .

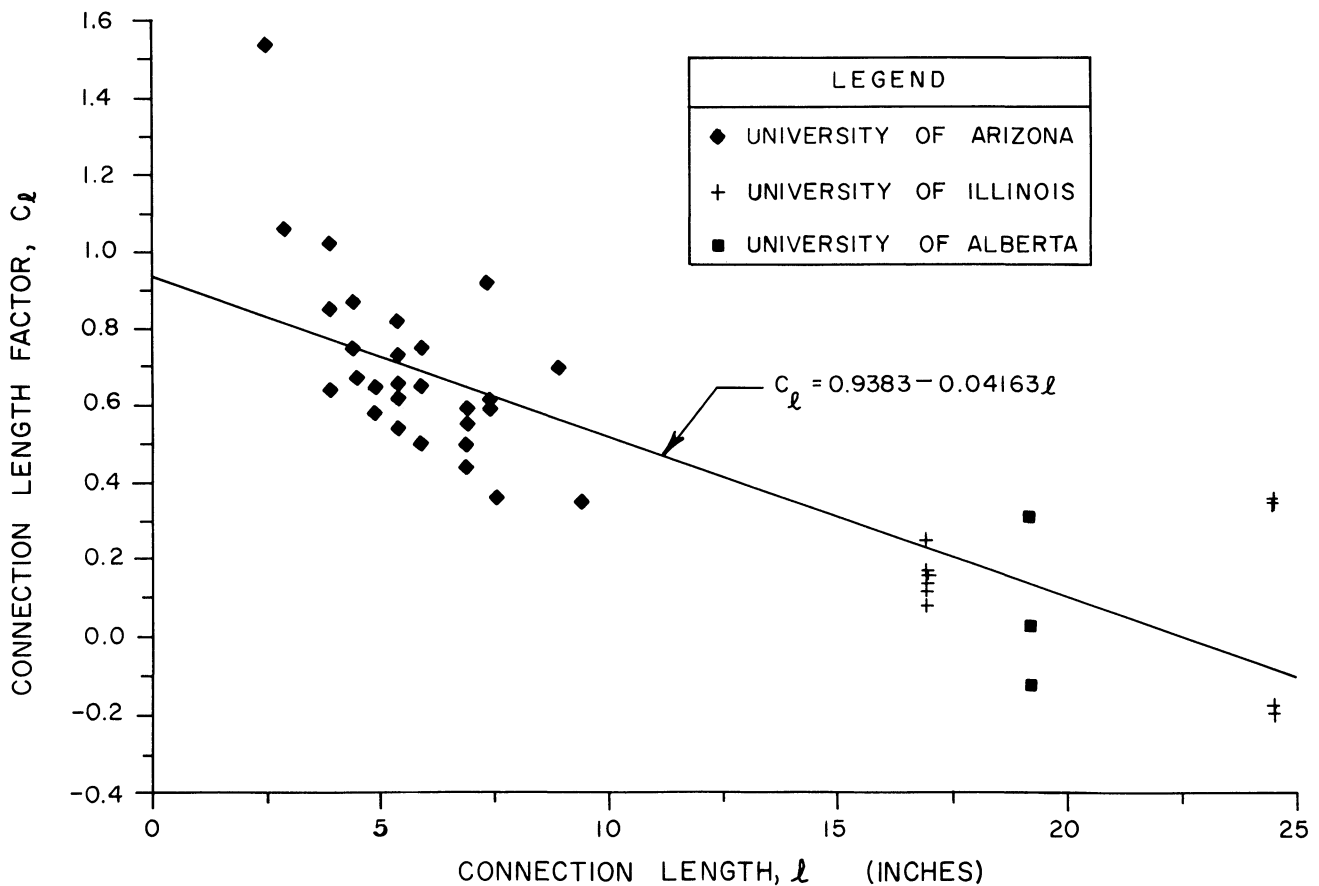


Fig. 13. Relationship between connection length factor,  $C_l$ , and connection length (42 tests)

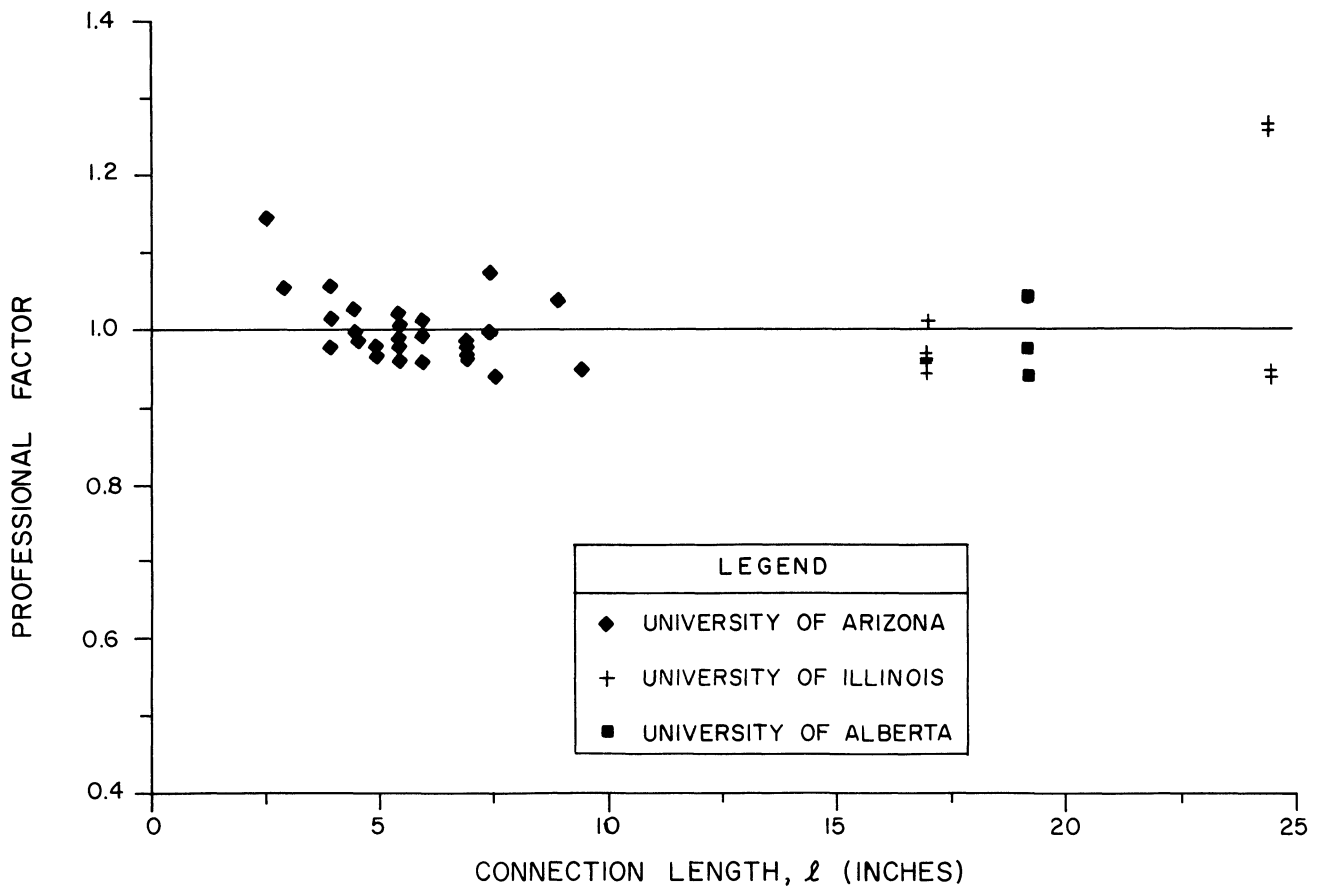


Fig. 14. Values of the professional factor vs. connection length, using 42 data points

Many possible curves could be fit through the points, but a least squares linear regression has been used for this study. The equation of this line in Fig. 13 is:

$$C_l = 0.9383 - 0.04163 \times l \quad (4)$$

where:

$C_l$  = Connection length factor to be used in Eq. 3

$l$  = Total connection length, in. (Note that Eq. 4 must be rephrased if metric units of length are used.)

It is interesting to note that for very short connections, a value of  $F_{eff}$  approaching  $F_u$  is obtained, and for connections longer than 22.5 in. (572 mm), the value for  $F_{eff}$  is less than  $F_y$ . This result appears intuitively correct, since longer connections would tend not to slip into bearing at mid-length of the connection.

Using Eq. 4 to determine the connection length factor, the effective uniform shear stress, expressed in terms of the effective tensile stress, can be obtained from Eq. 3. Using this effective stress in Eq. 2b, the theoretical ultimate strength can be obtained. Figure 14 shows the re-

sulting professional factor vs. connection length; the results of this figure can be compared to the data in Fig. 12b. For the 28 gusset plates tested during the present study, the mean value for the professional factor  $P$  is 1.000, with a coefficient of variation  $V_p$  of 0.0439. For all 42 tests,  $P_m$  is 1.003 with a coefficient of variation of 0.0716.

### Refinement of Strength Model

Figure 14 shows three of the 42 test plates exhibited much larger observed strengths than would be expected. Test plate No. 1 had almost the same observed strength as plate No. 2, although the only difference between the two was that plate No. 1 had an edge distance 0.40 in. (10 mm) less than No. 2. It is believed that since plate No. 1 was the first to be tested, some testing error might have evolved. Test plates Nos. 39 to 42 were plates with similar geometry and material, but the fabrication of plates Nos. 39 and 40 involved drilling of the bolt holes, while the holes were punched for Nos. 41 and 42. The 34% strength increase for the drilled specimens cannot be attributed completely to the hole preparation, as other

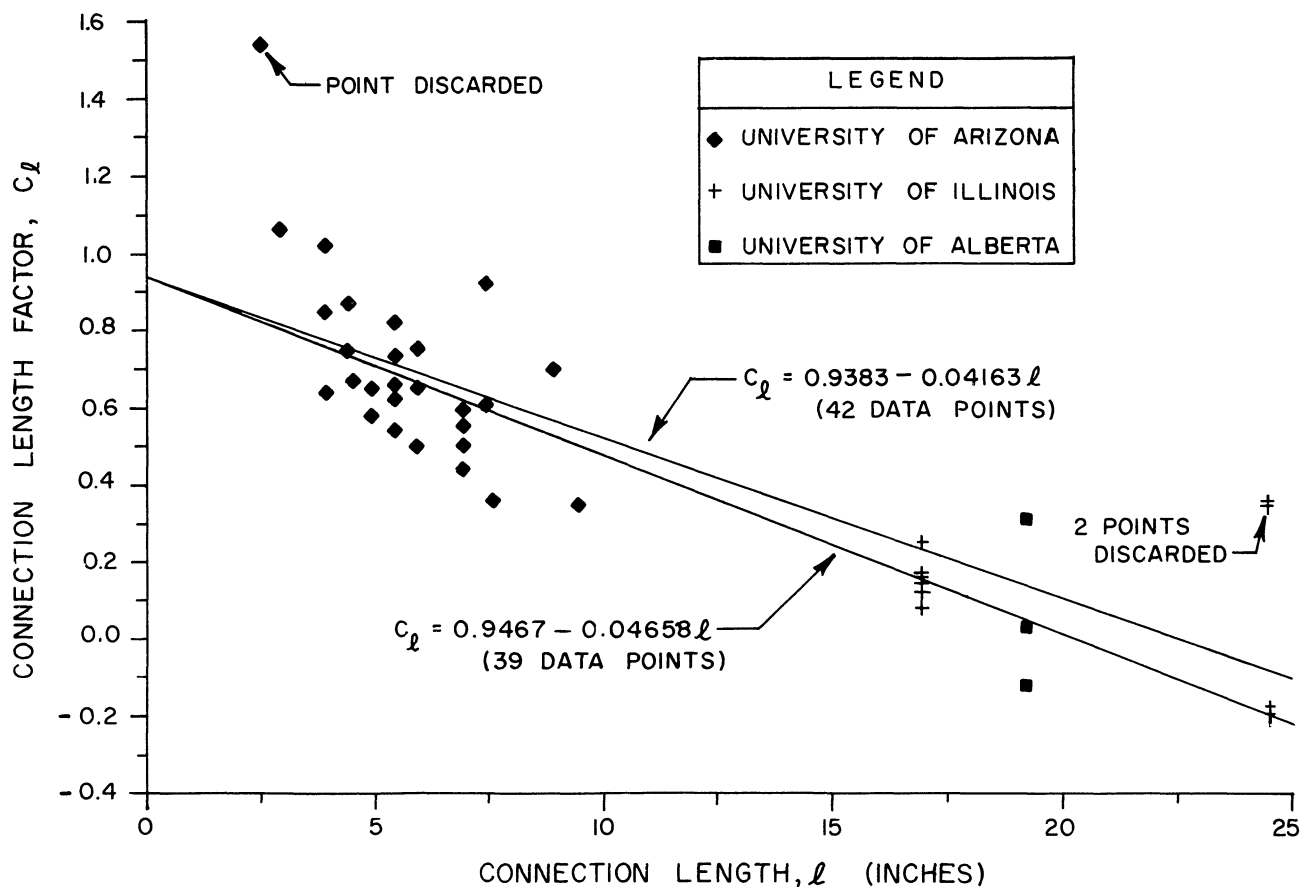


Fig. 15. Linear regression lines for the connection length factor, using 39 and 42 data points

identical plates with punched or drilled holes only showed a slight increase in strength (5%) for the drilled specimens. Based on these evaluations, it is justifiable to discard the results from test plate Nos. 1, 39 and 40, since they introduce test parameters not quantifiable and comparable to the other plates.

Figure 15 shows the regression line that has been developed on the basis of the remaining 39 gusset plate test results and the expression for the connection length factor is given as:

$$C_l = 0.9467 - 0.04658l \quad (5)$$

Using this expression for  $C_l$  to determine the effective shear stress, Eq. 2b can be used to obtain the theoretical strength.

The professional factor for each of the remaining 39 tests is plotted in Fig. 16. The mean value of  $P$  for the remaining 27 of the University of Arizona test results is 1.000, with a coefficient of variation of 0.0338. For all 39 tests,  $P_m$  is 1.001, with a coefficient of variation of 0.0322. This can be compared to the values of  $P_m = 1.003$  and  $V_p = 0.0716$  for all 42 tests.

The effects of the other strength parameters, both those directly used in the equations and those not included, were analyzed to determine if any additional relationships exist.<sup>11</sup> It has been concluded the effect of each strength parameter contained in the proposed block-shear equations is properly considered, and no others need be included.

To simplify the proposed equations, all constants should be rounded off to two decimal places. This results in the following set of equations, which gives the nominal ultimate resistance of a gusset plate loaded in tension:

$$R_n = F_u S_{net} t + 1.15 F_{eff} l t \quad (6)$$

$$F_{eff} = (1 - C_l) F_y + C_l F_u \quad (7)$$

$$C_l = 0.95 - 0.047 l \quad (8)$$

where:

- $R_n$  = Nominal ultimate resistance of connection
- $S_{net}$  = Net gage between outside bolts  
=  $S - (\text{no. of holes} - 1) \times \text{hole diameter}$
- $t$  = Plate thickness

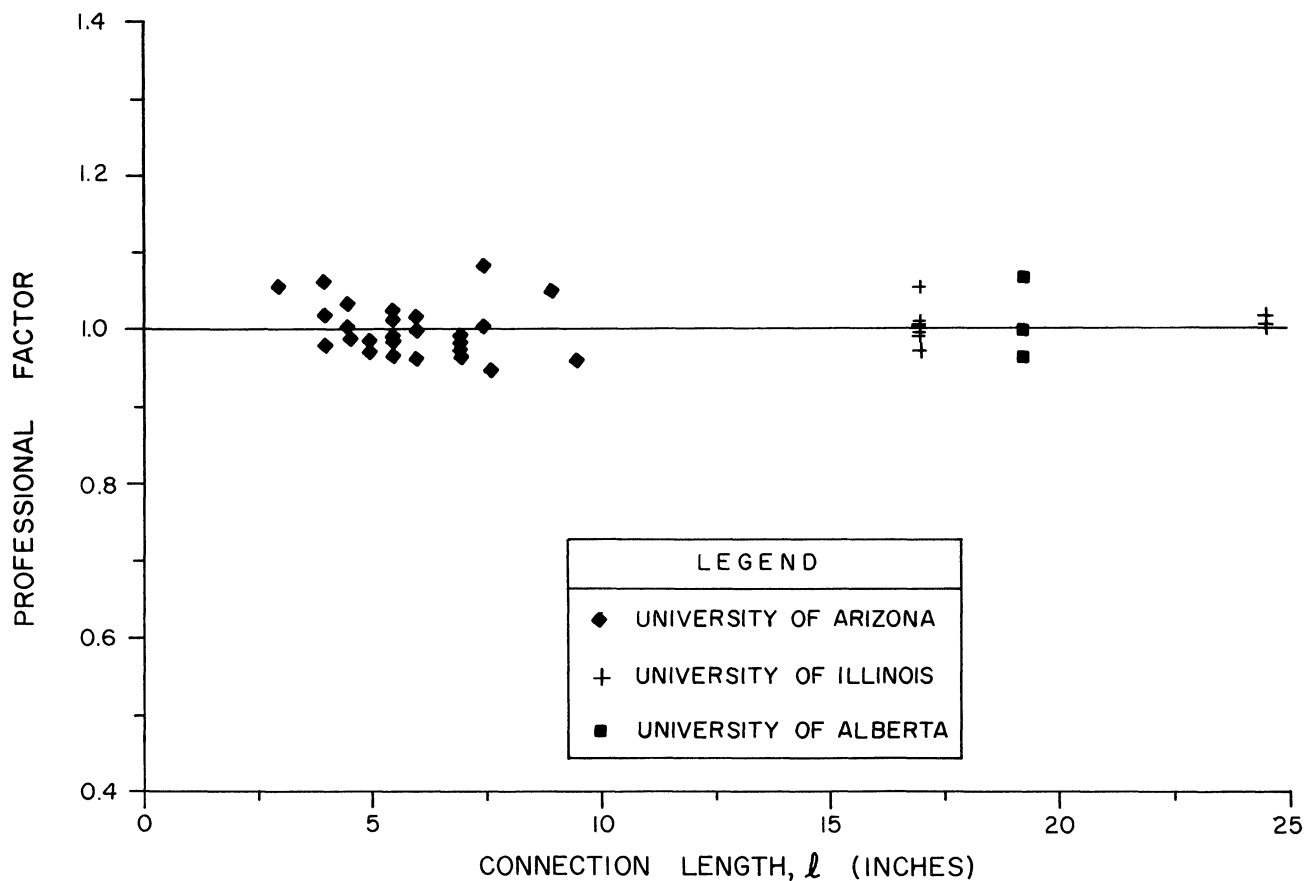


Fig. 16. Values of the professional factor vs. the connection length, using 39 data points

This simplification of the original equation changes the professional factor data only slightly, to  $P_m = 1.00$  and  $V_p = 0.033$ . It is therefore seen that performance of the model is excellent also in statistical terms, giving a low coefficient of variation, and a mean of 1.0 for results that reflect a wide range of strength parameters.

#### LOAD AND RESISTANCE FACTOR DESIGN OF GUSSET PLATES

##### Development of the Resistance Factor, $\phi$

The motivation behind developing an ultimate strength model for gusset plates is its eventual incorporation into a limit states design procedure. The development of the resistance factor will be presented in the following. For a more detailed treatment of the subject of LRFD, Refs. 8 to 10 give further documentation.

The mean strength  $R_m$  and the coefficient of variation  $V_R$  are given by the expressions:<sup>8,10</sup>

$$R_m = R_n P_m M_m F_m \quad (9)$$

$$V_r = \sqrt{V_p^2 + V_M^2 + V_F^2} \quad (10)$$

The coefficient  $P_m$  is the mean value of the professional factor, and the statistics of this term have been determined previously as  $P_m = 1.00$  and  $V_p = 0.033$ . The coefficient  $M_m$  represents the mean value of the ratio of the actual static yield stress to the specified minimum yield stress. The data for the statistics of this coefficient have been determined as  $M_m = 1.10$  and  $V_M = 0.11$ .<sup>9</sup> The coefficient  $F_m$  represents the mean value of the fabrication factor, and its statistics have been determined as  $F_m = 1.00$  and  $V_F = 0.05$ .<sup>8</sup> The fabrication factor is representative of the geometric accuracy of the component in question.

Incorporating the above data for  $M$ ,  $F$  and  $P$  and their coefficients of variation gives the following values for  $R_m$  and  $V_R$ , using Eqs. 9 and 10, respectively:

$$R_m = 1.10R_n$$

$$V_R = 0.125$$

The resistance factor,  $\phi$ , is given by the expression<sup>8,10</sup>

$$\phi = \frac{R_m}{R_n} \exp(-0.55 \beta V_R) \quad (11)$$

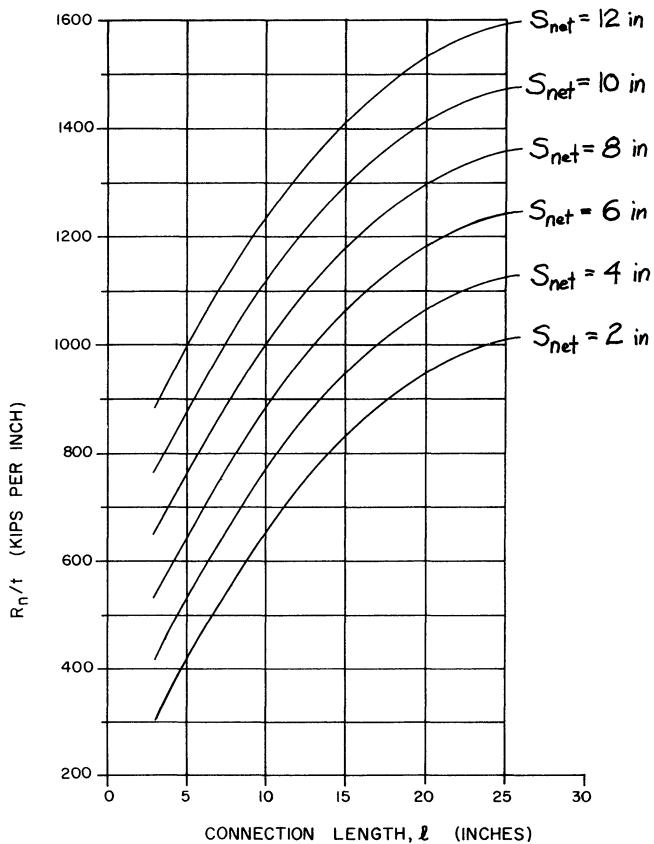


Fig. 17. Gusset plate design curves for ASTM A36 steel plate material

All terms in Eq. 11 have been determined in the preceding, except  $\beta$ , which represents the reliability index; an increasing value of  $\beta$  represents a decreasing probability of failure. It has been considered good practice to make connections stronger than the parts being joined, to give ample warning of impending failure. On this basis, connections in general have been assigned a value of  $\beta = 4.5$ , while the members they connect (beams, columns, etc.) have been assigned a value of  $\beta = 3.0$ .<sup>6</sup> Both of these values of  $\beta$  will be used to calculate  $\phi$  to obtain a range of values for this factor. From Eq. 11, the values for  $\phi$  are:

$$\text{For } \beta = 4.5: \phi = 0.81$$

$$\text{For } \beta = 3.0: \phi = 0.89$$

A suitable value would depend on the level of reliability that is needed. For example,  $\phi = 0.85$  appears to be a reasonable choice.

### Gusset Plate Design Curves

The proposed strength model lends itself well to the preliminary design of gusset plates. For instance, Eqs. 6, 7

and 8 can be combined into one expression, relating the plate thickness to the variables  $R_n$ ,  $S_{net}$ ,  $l$ ,  $F_y$ , and  $F_u$ . For a given type of steel,  $F_y$  and  $F_u$  are known, so the expression relates the gusset plate thickness directly to nominal strength  $R_n$  and the connection size  $S_{net}$  and  $l$ .

The above concepts have been applied to gusset plates of ASTM A36 steel [ $F_y = 36$  ksi (248 MPa) and  $F_u = 58$  ksi (400 MPa)], and the resulting curves are shown in Fig. 17 in which  $R_n/t$  has been plotted as a function of  $l$  and  $S_{net}$ . The result is a family of parabolas, since the strength model is a function of  $l^2$ . Interpolation between parabolas (fixed values for  $S_{net}$ ) is linear, since the strength model is a linear function of  $S_{net}$ . These design curves can be constructed for any type of steel, but A36 is probably the steel grade most commonly used for detail material.

Figure 17 shows that as the length of a connection increases, the rate of increasing gusset plate capacity decreases. This suggests that for longer connections it is more efficient to increase the outside bolt gage ( $S_{net}$ ). Figure 17 can be used in either of two ways: (1) if  $t$  has previously been chosen, then the connection size ( $l$  and  $S_{net}$ ) can be determined; or (2) if the connection size has been determined, then the necessary gusset plate thickness can be obtained. Either way, many combinations of gusset plate thickness and connection size can be checked quickly to determine the best design for the gusset plate connection.

**Design Example.** For illustration, consider the design of the gusset plate connection shown in Fig. 18. It has been found that two angles  $8 \times 6 \times 1/2$  with 12 A325 bolts in two lines (six bolts per line) will be adequate, using the proposed LRFD Specification.<sup>13</sup> To aid in the gusset plate design, it has also been determined that the minimum connection length for spacing requirements is 14.5 in. (368 mm), and the possible range of  $S_{net}$  is 1.4375 in. (36.5 mm)  $\leq S_{net} \leq$  4.6875 in. (119 mm), due to spacing requirements.<sup>13</sup> Many combinations are possible, but the maximum value for  $S_{net}$  will be used. With  $l = 14.5$  in. (368 mm) and  $S_{net} = 4.6875$  in. (119 mm), Fig. 17 gives a value of  $R_n/t = 970$  kips/in (170 kN/mm). Therefore:

$$\frac{\sum \gamma_i Q_{ni} = 490}{t} \leq \frac{\phi R_n}{t} = 970 \text{ kips-in.}$$

A value of  $\phi = 0.85$  as determined previously is used to obtain the necessary plate thickness:

$$t \geq \frac{490}{\phi 970} = \frac{490}{(0.85)970} = 0.594 \text{ in. (15.1 mm)}$$

Therefore, a gusset plate thickness of  $5/8$  in. (0.625 in., 16 mm) is adequate, and a total connection length of 14.5 in. (368 mm) and an outside bolt gage of 5.5 in. (140 mm) could be used.

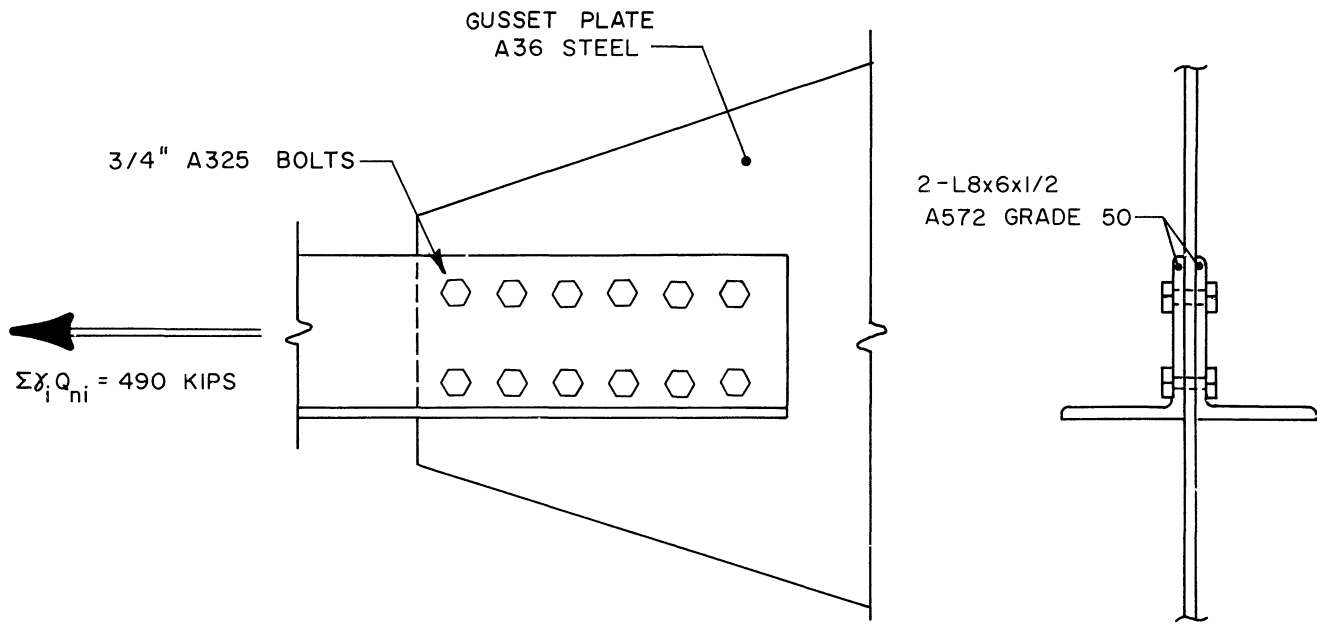


Fig. 18. Details of gusset plate connection for design example

If a thinner gusset plate is needed, say,  $\frac{9}{16}$  in. (14 mm), the required value of  $R_n/t$  is:

$$\frac{\sum \gamma_i Q_{ni}}{\phi t} = \frac{490}{(0.85)(9/16)}$$

$$= 1,025 \text{ kips/in. (180 kN/mm)} \leq \frac{R_n}{t}$$

With this value for  $R_n/t$  and  $S_{net} = 4.6875$  in. (119 mm), Fig. 17 gives the required total length as  $l = 16.5$  in. (419 mm).

The design with the  $\frac{9}{16}$ -in. thick gusset plate will now be checked. From Eq. 8,

$$C_l = 0.95 - 0.047(16.5) = 0.175$$

The effective stress becomes, from Eq. 7,

$$F_{eff} = (1 - 0.175)(36) + (0.175)(58)$$

$$= 39.9 \text{ ksi (275 MPa)}$$

The nominal strength is given by Eq. 6 as:

$$R_n = (58)[5.5 - (13/16)](9/16)$$

$$+ (1.5)(39.9)(16.5)(9/16)$$

$$= 578.8 \text{ kips (2576 kN)}$$

By the LRFD criterion,  $\sum \gamma_i Q_{ni} \leq R_n$ :

$$490 \text{ kips} \leq (0.85)(578.8 \text{ kips}) = 492 \text{ kips}$$

Therefore, the gusset plate thickness and connection size are adequate.

The above computations demonstrate the ease with which gusset plate connections can be sized using the proposed procedure. Naturally, for the complete connection design, the limit state of yielding on the gross cross-section just below the last row of bolts and the limit state of tensile failure on the net section at the last row of bolts must also be checked.

## SUMMARY AND CONCLUSIONS

This paper has presented the following observations and conclusions for tensile gusset plate connections:

1. All ultimate failure modes consist of a tensile tear across the last row of bolts, with various stages of shear yielding along the outside lines of bolts. The extent of the latter depends on the connection length.
2. The governing block-shear model is shown to be the one incorporating tensile ultimate stress on the net area between the last row of bolts, and a uniform effective shear stress acting on the gross area along the outside bolt lines.
3. The effective shear stress acting along the outside bolt lines can be assumed to be uniformly distributed, with the magnitude given as a function of the total connection length, and material yield and ultimate stress levels.

From the above, three equations have been developed which accurately predict the ultimate strength of 39 gusset plate tests. The accuracy of the proposed model is not affected by such factors as plate boundaries, fastener

size or edge distance to the first bolt line.

Typical design curves for A36 steel are presented to demonstrate the ease with which tensile gusset plate connections can be sized and gusset plate thicknesses selected to give maximum connection efficiency.

The 39 gusset plate tests considered in the development of the final strength model have included a wide range of strength parameters. However, it may prove worthwhile to conduct additional tests, especially with connection lengths within the range of 10 to 16 in. (254 to 406 mm).

This study did not address the problems of compressive gusset plate connections, nor the related problem of gusset plate buckling, which are important future considerations. Also, the combined effect of multiple members framing into one gusset plate, and gusseted connections in close proximity to boundary elements are important areas to investigate further.

#### ACKNOWLEDGMENTS

The work presented in this paper formed part of a research project funded by the American Institute of Steel Construction, Inc. Special thanks are due the Institute for this support, as well as the individuals who assisted in the research. Messrs. M. F. Leong and A. E. Moussa provided invaluable work in the laboratory, and the shop work of Messrs. W. D. Lichtenwalter and L. Lujan was essential to the success of the work. Mrs. Carole Goodman did an excellent job in typing of the manuscript.

#### NOMENCLATURE

|              |   |
|--------------|---|
| $A_t$        | = net tension area                        |
| $A_v$        | = net shear area                          |
| $C_l$        | = connection length factor                |
| $e$          | = edge distance                           |
| $F_{eff}$    | = effective tensile stress                |
| $F_m$        | = mean value of the fabrication factor    |
| $F_u$        | = ultimate tensile strength               |
| $F_y$        | = tensile yield stress                    |
| $l$          | = total connection length                 |
| $l_{net}$    | = net connection length                   |
| $M_m$        | = mean value of the material factor       |
| $P$          | = professional factor                     |
| $P_m$        | = mean value of the professional factor   |
| $P_{theory}$ | = theoretical block-shear capacity        |
| $Q$          | = generalized load effect                 |
| $R_a$        | = nominal resistance to block-shear       |
| $R_m$        | = mean resistance                         |
| $R_n$        | = nominal resistance                      |
| $s$          | = bolt pitch                              |
| $S$          | = gage between outside bolt lines         |
| $S_{net}$    | = net distance between outside bolt lines |
| $t$          | = gusset plate thickness                  |

|              |   |
|--------------|---|
| $V_F$        | = coefficient of variation of fabrication uncertainties |
| $V_P$        | = coefficient of variation of theoretical assumptions   |
| $V_R$        | = coefficient of variation of resistance                |
| $\beta$      | = reliability index                                     |
| $\gamma$     | = load factor   |
| $\tau$       | = shear stress  |
| $\tau_{eff}$ | = effective shear stress                                |
| $\phi$       | = resistance factor                                     |

#### REFERENCES

1. Annual Book of ASTM Standards *ASTM, Section 1, Vol. 01.04, Easton, Md., 1984.*
2. Birkemoe, P. C. and M. I. Gilmore Behavior of Bearing Critical Double-Angle Beam Connections *AISC Engineering Journal, 4th Qt., 1978, pp. 109-115.*
3. Bjorhovde, Reidar and S. K. Chakrabarti Tests of Gusset Plate Connections *Research Report, Dept. of Civil Engineering, Univ. of Arizona-Tucson, April 1983.*
4. Chesson, E., Jr. and W. H. Munse Behavior of Riveted Truss-Type Connections *ASCE Transactions, Vol. 123, 1958, pp. 1,087-1,128.*
5. Chesson, E., Jr. and W. H. Munse Riveted and Bolted Joints: Truss-Type Tensile Connections *ASCE Journal of the Structural Division, Vol. 89, No. ST1, February 1963, pp. 67-106.*
6. Fisher, J. W., T. V. Galambos, G. L. Kulak and M. K. Ravindra Load and Resistance Factor Design Criteria for Connectors *ASCE Journal of the Structural Division, Vol. 104, No. ST9, September 1978, pp. 1,427-1,441.*
7. Fisher, J. W. and J. H. A. Struik Guide to Design Criteria for Bolted and Riveted Joints *John Wiley and Sons, Inc., New York, N.Y., 1974.*
8. Galambos, T. V. and M. K. Ravindra Load and Resistance Factor Design for Steel *ASCE Journal of the Structural Division, Vol. 104, No. ST9, September 1978, pp. 1,337-1,353.*
9. Galambos, T. T. and M. K. Ravindra Properties of Steel for Use in LRFD *ASCE Journal of the Structural Division, Vol. 104, No. ST9, September 1978, pp. 1,459-1,468.*
10. Galambos, T. V. Load and Resistance Factor Design *AISC Engineering Journal, 3rd Qt., 1981, pp. 74-82.*
11. Hardash, S. G. and Reidar Bjorhovde Gusset Plate Design Utilizing Block-Shear Concepts *Research Report, Dept. of Civil Engineering, Univ. of Arizona-Tucson, August 1984.*
12. American Institute of Steel Construction, Inc. Manual of Steel Construction *8th Ed., 1980, Chicago, Ill.*
13. American Institute of Steel Construction, Inc. Proposed Load and Resistance Factor Design Specification for Structural Steel Buildings *Sept. 1, 1983, Chicago, Ill.*

14. Rabern, D. A. Stress, Strain and Force Distributions in Gusset Plate Connections *Thesis presented to the Univ. of Arizona-Tucson, 1983, in partial fulfillment of the requirements for the degree of Master of Science in Civil Engineering.*
  15. Richard, R. M., D. A. Rabern, D. E. Hormby and G. C. Williams Analytical Models for Steel Connections *Behavior of Metal Structures, Proceedings of the W.H. Munse Symposium, W. J. Hall and M. P. Gaus, Eds., ASCE, May 17, 1983, pp. 128–155.*
  16. Ricles, J. M. and J. A. Yura Strength of Double-Row Bolted-Web Connections *ASCE Journal of the Structural Division, Vol. 109, No. 1, January 1983, pp. 126–142.*
  17. Canadian Standards Association Steel Structures for Buildings—Limit States Design *CSA Standard S16.1-1974, Rexdale, Ontario, Canada, December 1974.*
  18. Struik, J. H. A. Applications of Finite Element Analysis to Nonlinear Plane Stress Problems *Thesis presented to Lehigh Univ., Bethlehem, Pa., 1972, in partial fulfillment of the requirements for the degree of Doctor of Philosophy in Civil Engineering.*
  19. Whitmore, R. E. Experimental Investigation of Stresses in Gusset Plates *Univ. of Tennessee Engineering Experiment Station Bulletin 16, May 1952.*
  20. Yura, J. A., P. C. Birkemoe and J. C. Ricles Double Angle Beam Web Connections: An Experimental Study *ASCE Journal of the Structural Division, Vol. 108, No. ST2, February 1982, pp. 311–325.*
-